DESIGN OF A 1 kHz REPETITION RATE S-BAND PHOTOINJECTOR

Jang-Hui Han, Diamond Light Source, Oxfordshire, United Kingdom.

Abstract

S-band photoinjectors operate to provide high quality beams at many laboratories, however the repetition rates are limited to about 100 Hz. This limitation mainly results from the guns where an RF amplitude of about 100 MV/m is required to keep the beam quality against the space charge force. In this paper we design an injector consisting of an S-band gun with improved cooling and S-band accelerating sections for a repetition rate of 1 kHz.

INTRODUCTION

Previous work on S-band gun resulted in a design which would be capable of operation at 400 Hz with a peak RF field at the cathode of 120 MV/m [1]. Here we present the design of a gun which will operate with a 1 kHz repetition rate when a 100 MV/m RF peak field at the cathode and a 3 μs RF pulse length are used [2], while still providing similar beam parameters. At the same time, more conservative input parameters in the drive laser rise/fall time and in the thermal emittance were used in this study.

By using this high repetition gun, an S-band injector for a free electron laser (FEL) has been designed aiming at a 1 kHz operation for the entire injector. In addition, beam generation with a short bunch length was considered so that the electron beam can be further accelerated with C- or X-band accelerating cavities after the injector if the injector is followed by a magnetic bunch compressor. Several FEL projects using such high resonance frequency cavities for beam acceleration are ongoing or under preparation to reduce the total length of the linac and also reduce costs [3, 4, 5].

INJECTOR LAYOUT

Photocathode RF gun

This gun has a coaxial RF coupler as adopted at the PITZ gun [6] so that the cooling capacity is maximal and the focusing solenoid can be placed at an optimum position for the so-called emittance compensation process [7], which is around the second cell of the gun [6]. For most S-band guns, the RF peak field is around 120 MV/m. In general, a high RF field helps to preserve the beam quality against the space charge force. However, a high RF field requires a high RF power and limits the repetition rate. A high field at the cathode also increases the kinetic energy of photoemitted electrons and therefore the thermal emittance of the beam increases. A high RF field in the gun also generates a high level of dark current. In this design, the RF peak field is set to 100 MV/m.

Accelerating sections

After the beam is photoemitted and accelerated up to 4.2 MeV at the gun, the beam is further accelerated to be fully relativistic. Four 3.1 m long constant gradient accelerating cavities are used. To allow a 1 kHz repetition rate operation, the gradient of the four cavities was set to 12 MV/m, which was scaled down from a 20 MV/m gradient for 400 Hz as discussed in [8] to keep the same average power burden to the RF sources and cavities.

Solenoids

The position of the main gun solenoid was one of the optimization parameters and was set to 0.11 m from the cathode. A bucking solenoid compensates the magnetic field at the cathode so that the beam angular momentum does not increase the transverse emittance after the gun solenoid field.

At each accelerating sections focusing solenoids are used to control the beam size and keep the transverse emittance.

Initial beam generation for simulation

The drive laser pulse length was fixed to 7 ps for all bunch charge cases. Shorter pulse lengths were tried but the transverse emittance increased significantly. The rise/fall time of the laser pulse was 1 ps. A uniform transverse beam shape was used. The radius was one of the optimization variables.

A photon energy of about 4.9 eV and a metal cathode (Cu or Mo) which has a work function of about 4.6 eV [9] were assumed. Then, the kinetic energy of photoemitted electrons was set to be 0.6 eV considering the Schottky effect and other possible sources such as cathode surface roughness and laser pulse inhomogeneity. The thermal emittance is, consequently, 0.443 mm mrad per 1 mm full radius of the initial beam.

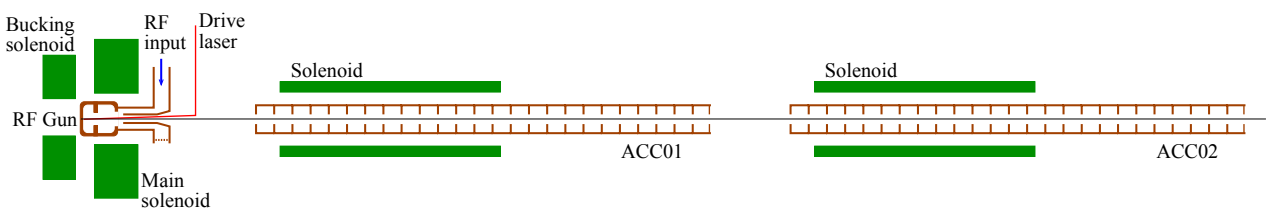

Figure 1: Injector layout. It consists of an S-band photocathode gun, a drive laser, four accelerating sections, and focusing magnets. The last two sections (ACC03 and ACC04) are not shown here.

INJECTOR BEAM DYNAMICS

The cavity and solenoid field profiles were calculated with POISSON/SUPERFISH [10]. Using the field profiles, the beam dynamics was simulated with ASTRA [11]. Gun phase, position and phase of the accelerating cavities (ACC01 – ACC04) and position and field strength of the solenoids were used as optimization parameters. For optimization iterations, 10,000 macro-particles were used for ASTRA simulation. For the results discussed below, 100,000 macro-particles were used.

To minimize beam degradation due to the space charge force, a relatively long bunch (7 ps fwhm) was generated at the cathode and accelerated with 100 MV/m peak field at the gun. When the beam reaches 4.2 MeV after the gun, a mild velocity bunching was applied with ACC01. Figure 2 shows the beam energy and bunch length evolution through the injector.

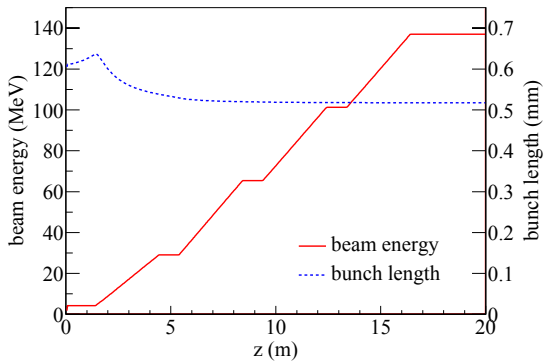

Figure 2: Beam energy and bunch length for a 50 pC beam. By the velocity bunching with ACC01 the bunch length decreases by about 20%.

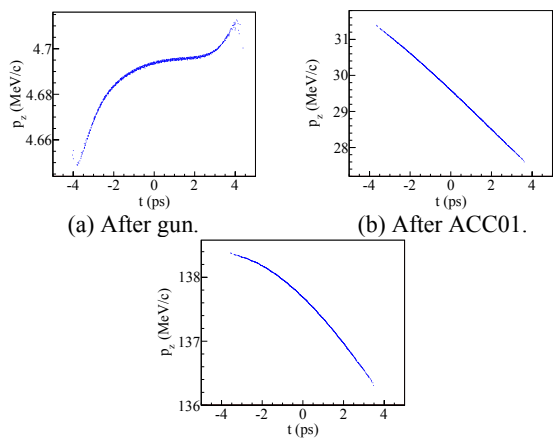

(a) After gun. (b) After ACC01.

(c)After ACC04.

Figure 3: Longitudinal phase space for a 50 pC beam.

When an electron beam exits the gun, the longitudinal phase space is configured, due to the space charge force, so that the head has a higher energy and the tail has a lower energy (Fig. 3a). As the beam propagates, the bunch length therefore becomes longer. The space charge expansion may be reduced if the initial bunch length is long or the transverse beam size is larger. However, both of these options are not preferred because we want to have a high peak current and a low initial beam emittance. This dilemma may be solved with a small initial beam size but a long initial length. A mild velocity bunching is then applied at the first part of ACC01 (Fig. 3b) while the beam is accelerated so that beam degradation does not occur. The phase of ACC01 was set to –50° from the on-crest phase. The energy chirp produced during the velocity bunching may be controlled with other accelerating cavities downstream (Fig. 3c). Once the beam becomes fully relativistic, the beam quality is not affected by the accelerating cavity phase. The input parameters for the simulation are listed in Table 1.

Table 1: Simulation input parameters of laser, gun, linac and solenoid and the simulation results with ASTRA for 20 pC, 50 pC and 200 pC beams. The parameters shown below are after ACC04.

Parameters	20 pC	50 pC	200 pC
Laser			
pulse length (ps)	7	7	7
rise/fall time (ps)	1	1	1
radius (mm)	0.12	0.20	0.38
E_{kin} of emitted e^- (keV)	0.6	0.6	0.6
thermal ε (mm mrad)	0.0531	0.0885	0.168
Gun			
peak field (MV/m)	100	100	100
phase from on-crest (deg)	–2	–2	–2
Accelerating Sections			
grad. at all ACCs (MV/m)	12	12	12
phase at ACC01 (deg)	–50	–50	–50
phase at ACC02 (deg)	0	0	0
phase at ACC03 (deg)	10	10	10
phase at ACC04 (deg)	10	10	10
Solenoids max field			
at gun main (T)	0.321	0.321	0.321
at ACC01 (T)	0.035	0.045	0.045
at ACC02 (T)	0.075	0.07	0.06
at ACC03 (T)	0.085	0.07	0.055
at ACC04 (T)	0.085	0.07	0.055
Beam at the end of injector			
100% proj. ε (mm mrad)	0.062	0.103	0.231
central slice ε (mm mrad)	0.056	0.095	0.197
beam size (mm)	0.095	0.121	0.230
bunch length, fwhm (ps)	5.5	6	7.3
peak current (A)	4	9	30
$\Delta E/E$ at center	3.3×10^{-6}	2.4×10^{-6}	5.2×10^{-6}
mean E (MeV)	137	137	137

The temporal distributions of beams at three bunch charge (20 pC, 50 pC, and 200 pC) are shown in Fig. 4. Even though we used the same initial bunch length from the cathode (7 ps) and the same RF parameters at the gun and the accelerating cavities, the bunch lengths at the end of the injector are not the same because of the different space charge forces.

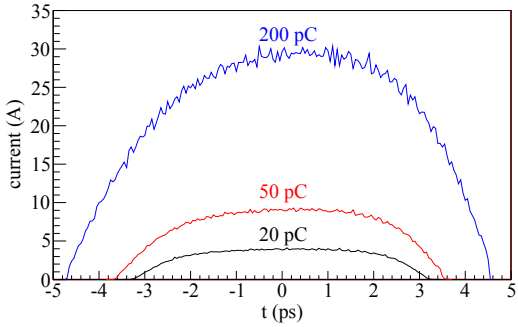

Figure 4: Temporal profiles after ACC04. Three bunch charge cases, 20 pC, 50 pC, and 200 pC, are shown.

To control the transverse emittance and beam size, ACC01 was set to start at 1.35 m. The emittance at the end of the injector depends significantly on the position of ACC01. ACC02 was placed at 0.9 m downstream of the exit of ACC01, however this position is not crucial. For the installation of diagnostics, ACC02 (and also ACC03 and ACC04) can be placed flexibly. The normalized transverse emittance and beam size for a 50 pC beam are shown in Fig. 5. Slice emittances for the three bunch charge cases at the end of injector are shown in Fig. 6.

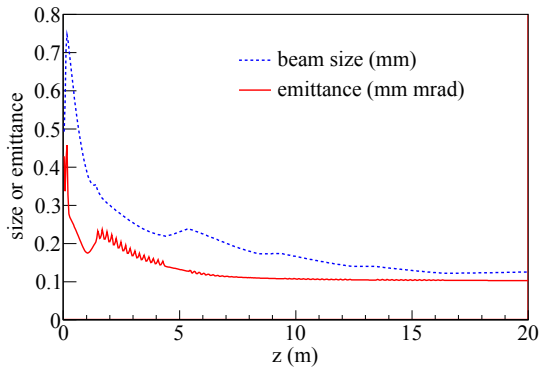

Figure 5: Transverse beam size and 100% projected normalized emittance for a 50 pC beam.

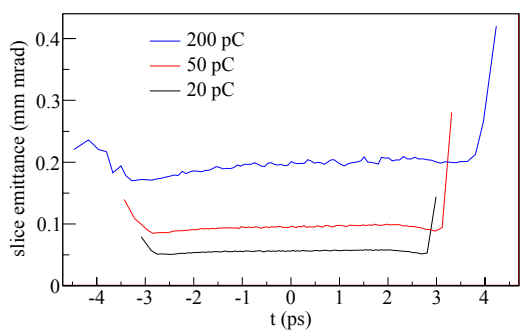

Figure 6: Slice transverse emittances for the three bunch charge cases.

The slice energy spread at the end of the injector is below 1 keV (Fig. 7). A laser heater may be needed before the first magnetic bunch compressor to preserve the beam quality from the micro-bunching instability [12].

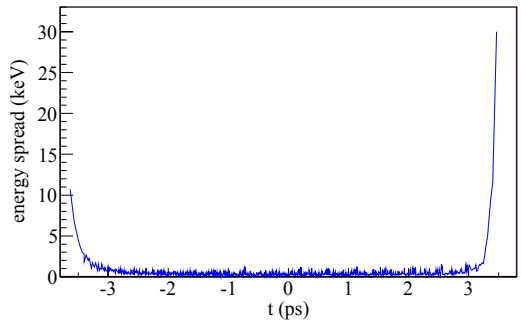

Figure 7: Slice energy spread for a 50 pC beam.

DISCUSSION

A low emittance S-band photoinjector has been designed capable of 1 kHz repetition rate operation. The water-cooling capacity was enlarged and the gun peak field was set to 100 MV/m. The gradient of the accelerating cavities was set to 12 MV/m. With a thermal emittance of 0.443 mm mrad per 1 mm full radius considered, a normalized slice emittance about 0.2 mm mrad will be achievable at 200 pC. Injector optimization was also carried out for 50 pC and 20 pC cases.

As default, a metal cathode was assumed to be used for beam generation. However, since an exchangeable cathode plug is included in the gun design, there is flexibility to choose the cathode material. For example, for a high charge option, Cs-Te may be coated on the metal plug.

ACKNOWLEDGEMENTS

JHH thanks R. Bartolini, C. Christou, and R. Walker for fruitful discussions.

REFERENCES

[1] J.-H. Han, These Proceedings, THP104.
[2] T. Shintake, IPAC10, p. 1258.
[3] T. Garvey, FEL10, MOOB3.
[4] C. Adolphsen, Workshop on X-band RF Technology for FELs, SLAC, 2010.
[5] J.-H. Han, LINAC08, TUP099, p. 636.
[6] B. Dwersteg et al., Nucl. Instr. and Meth. A **393**, 93 (2997).
[7] B. E. Carlsten, Nucl. Instr. and Meth. A **285**, 313 (1989).
[8] C. Christou et al., LINAC08, p. 462.
[9] D. E. Eastman, Phys. Rev. B **2**, 1 (1970).
[10] J.H. Billen and L.M.Young, "Poisson Superfish", LAUR-96-1834.
[11] K. Floettmann, "A Space Charge Tracking Algorithm (ASTRA)", http://www.desy.de/~mpyflo.
[12] Z. Huang et al., Phys. Rev. ST Accel. Beams **7**, 074401 (2004).